Swain et al. Ecological Processes (2015) 4:4
DOI 10.1186/s13717-014-0028-3

Ecological Processes
a SpringerOpen Journal

RESEARCH Open Access

Numerical computation of hurricane effects on historic coastal hydrology in Southern Florida

Eric D Swain[1*], Dennis Krohn[2] and Catherine A Langtimm[3]

Abstract

Introduction: Numerical models are critical for assessing the effects of sea level rise (SLR), hurricanes, and storm surge on vegetation change in the Everglades National Park. The model must be capable of representing short-timescale hydrodynamics, salinity transport, and groundwater interaction. However, there is also a strong need to adapt these numerical models to hindcast past conditions in order to examine long-term effects on the distribution of vegetation that cannot be determined using only the modern record.

Methods: Based on parameters developed for a numerical model developed for the recent 1996 to 2004 period, a hindcast model was developed to represent sea level and water management for the period of 1926 to 1932, constrained by the limited hydrology and meteorology data available from the historic past. Realistic hurricane-wind and storm surge representations, required for the hindcast model, are based on information synthesized from modern storm data. A series of simulation scenarios with various hurricane representations inserted into both hindcast and recent numerical models were used to assess the utility of the storm representation in the model and compare the two simulations.

Results: The comparison of the hindcast and recent models showed differences in the hydrology patterns that are consistent with known differences in water delivery systems and sea level rise. A 30× lower-resolution spatially variable wind grid for the hindcast produced similar results to the original high-resolution full wind grid representation of the recent simulation. Storm effects on hydrologic patterns demonstrated with the simulations show hydrologic processes that could have a long-term effect on vegetation change.

Conclusions: The hindcast simulation estimated hydrologic processes for the 1926 to 1932 period. It shows promise as a simulator in long-term ecological studies to test hypotheses based on theoretical or empirical-based studies at larger landscape scales.

Keywords: Hindcast; Numerical models; Hurricanes; Wind fields; Storm surge; Sea level rise; Coastal hydrology

Introduction

Hurricanes and cyclones are major drivers of coastal ecological processes at all levels of biological organization from populations to communities to ecosystems and operate across a hierarchy of spatial and temporal scales (Michener et al. 1997). Hurricane and cyclone effects are receiving greater emphasis and study worldwide with recent high-profile devastating landfall storms (i.e., Hurricane Katrina 2005, Superstorm Sandy 2012, Super Typhoon Haiyan 2013) but also with climate change resulting in rising sea levels and intensification of tropical cyclones (Khairoutdinov and Emanuel 2013) with unpredictable potential effects.

Extensive research in the Greater Everglades, Florida, USA (Figure 1), conducted as part of the development of a major project to restore the historical hydrology of this unique system (http://www.evergladesplan.org/) has documented the role of changing sea levels and hurricane disturbance on the formation of the Everglades (Ogden et al. 2005; Obeysekera et al. 1999; Davis et al. 2005) and enhanced understanding of many coastal ecological processes. For example, empirical field studies identified the importance of storms on ecosystem structure and function in mangrove estuaries (Davis et al. 2004), the role of mangroves as buffers to storm surge (Zhang et al. 2012),

* Correspondence: edswain@usgs.gov
[1]U.S. Geological Survey, Caribbean-Florida Water Science Center, 7500 SW 36th Street, Davie, FL 33314, USA
Full list of author information is available at the end of the article

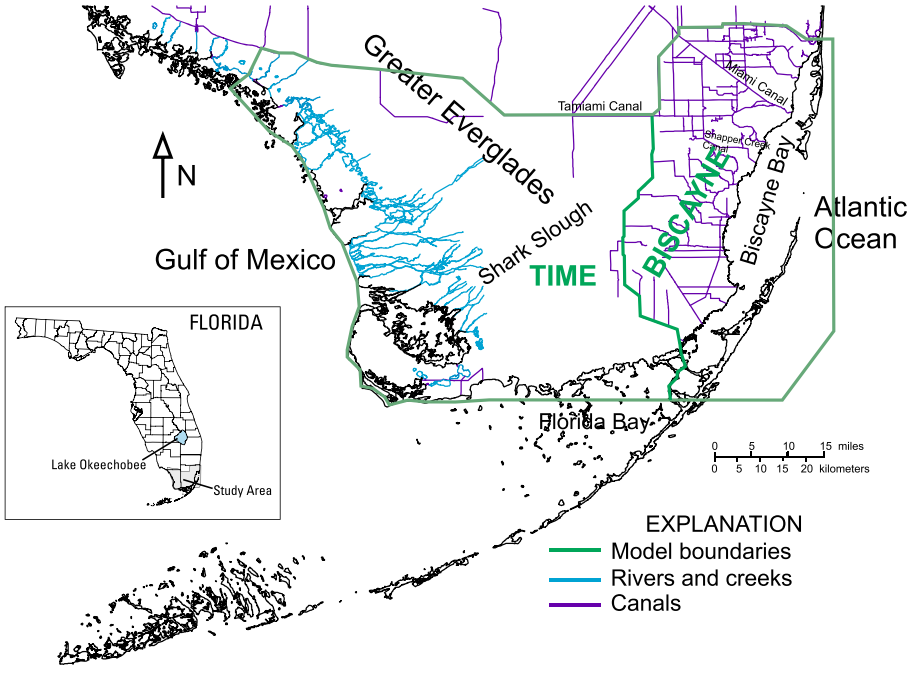

Figure 1 Study area in South Florida showing TIME and BISCAYNE model boundary and modern canal distribution.

and how storms and sea level rise affect sediment accretion and organic carbon burial rates (Smoak et al. 2013). Theoretical and empirical research on mangrove-marsh and mangrove-forest ecotones have identified processes important to non-linear system dynamics, which relate to ecosystem resilience, tipping points for vegetation regime change, and delayed ecosystem effects on the order of years after a particular salinity event (Teh et al. 2008; Jiang et al. 2012b; Jiang and DeAngelis 2013; Jiang et al. 2012a; Jiang et al. 2014). Results and findings specific to the Everglades have application worldwide. However, additional research is needed, particularly at larger spatial scales to address regional effects (Hopkinson et al. 2008; Heffernan et al. 2014) and at long temporal scales to address non-linear system dynamics due to propagating events within a hierarchy of ecological processes (Peters et al. 2007). Hopkinson et al. (2008) made the case for a continental network of coastal and inland observation sites to monitor and evaluate the influence of sea level rise and windstorms. Although field studies can provide short-term insights, they are limited in their insights to long-term dynamics. Hydrodynamic numerical models at large spatial scales offer a tool to simulate and study the effects of short-term events on long-term processes.

As part of a larger U.S. Geological Survey study focused on ecological interactions in the mangrove estuaries ecosystem fringing the Everglades, an existing numerical model is modified to represent hurricane disturbance. To investigate patterns and processes involved in long-term vegetation change, numerical models are used to simulate hydrologic conditions during the periods of 1926 to 1932 and 1996 to 2004 coincident with vegetation occurrence documented in geo-referenced aerial photos and charts (Smith et al. 2002; Smith et al. 2010). Retrospective analyses of the hindcast output (1926 to 1932) and a time series of past habitat types will be used to identify patterns of ecosystem change and generate and test hypotheses of long-term ecological-hydrological processes. Ultimately, the goal of further research would be to develop simulations of future hydrology to explore scenarios of climate change and adaptive management. However, to realistically simulate future ecological processes and outcomes, it is first necessary to develop a reliable hindcast that accurately reproduces the effects of major storm events.

Hydrodynamic simulation of hurricane storm surge can include complex three-dimensional flow and barotropic effects, as in the application of the CH3D-SSMS-integrated storm surge modeling system to the northeast Florida coast (Sheng and Paramygin, 2010). Circulation patterns and inundation are represented in a simulation of Tropical Storm Fay in 2008. When groundwater interactions are of interest, coupled surface-water/groundwater models of the South Florida area have been developed to examine coastal hydrology and related issues. The primary simulator developed for representing hydrodynamic surface-water flow coupled to groundwater in a highly porous aquifer is called Flow and Transport in a Linked Overland/Aquifer Density-Dependent System (FTLOADDS) (Langevin et al. 2005). FTLOADDS links the two-dimensional hydrodynamic flow and transport code SWIFT2D (Swain, 2005)

with the widely used three-dimensional groundwater flow and transport code SEAWAT (Guo and Langevin, 2002). Both regimes incorporate the effects of salinity concentration on water density. The capability to simulate surface-water heat transport and temperature was incorporated into the code with the added benefit of cell-by-cell evapotranspiration computations (Swain and Decker, 2010).

The FTLOADDS numerical simulator is needed to represent three unique aspects of the South Florida hydrology: (1) the low water-level gradients and flat topography, (2) the highly porous aquifer, and (3) salinity transport in both the surface-water and groundwater systems. The unique capability of FTLOADDS to simulate the full hydrodynamic solution, which is especially suited to dynamic events with substantial inertial forcing, allows for the representation of short-term surface-water transient effects such as tidal changes and wind-driven flux while simulating salinity mixing. With the SWIFT2D/SEAWAT linkage simulating the exchange of surface water with the groundwater, all the important controlling processes including tide, wind, precipitation, evapotranspiration, and surface-water management are represented. In comparison, a simpler surface-water/groundwater model does not have the ability to represent short-term hydrodynamic storm events and other transient phenomena while also simulating the impact of these short-lived and spatially explicit events on long-term and landscape-scale hydrodynamic processes, which are important to the resultant short- and long-term ecological response.

Two major applications developed with FTLOADDS are the TIME model of the Everglades National Park area (Wang et al. 2007) and the BISCAYNE model of the eastern urban area and Biscayne Bay (Lohmann et al. 2012). Together, these applications encompass the natural and urban areas of Miami-Dade County (Figure 1). The initial period of simulation was 1996 to 2002 but was later expanded to 1996 to 2004, incorporating a larger variety of annual hydrologic conditions (Swain and Lohmann, US Geological Survey, March 2014, written communication). Applications of FTLOADDS have been utilized to develop surface-water discharges for salinity targets (Swain and James, 2007), examine the effects of ecosystem restoration (Swain et al. 2008, Obeysekera et al. 2011), provide salinity and temperature estimates for manatee habitats (Stith et al. 2011), determine causes of hypersalinity in Biscayne Bay (Lohmann et al. 2012), represent the effects of hydrological restoration scenarios on American crocodiles (Green et al. 2014), and forecast the impact of future precipitation changes and sea level rise in coastal areas (Swain, Stefanova, and Smith, 2014).

TIME/BISCAYNE covers an area with a maximum extent of 93 km north-south and 129.5 km east-west. Each model cell is 0.5 × 0.5 km and approximately 55,000 grid cells cover the area. The groundwater simulation has a time step of 1 day whereas the surface water is simulated at a 10-min interval. Model inputs are defined in various time intervals: 30-min tidal levels, 6-h average rainfall, and 4-h average wind. However, the option exists to input spatially variable wind fields for specific periods at any desired time intervals, a useful option for representing storm events. Variables output by the model include groundwater and surface-water salinity, hydroperiod, flow, stage, depth, water temperature, and other time series.

There are several challenges involved in modifying TIME/BISCAYNE calibrated to the years 1996 to 2004 (recent) to develop a simulation of past conditions from 1926 to 1932 (hindcast).

1) The lower sea level during the hindcast period compared to recent times must be accounted for in the simulations. The coastal hydrology and inundation must be simulated correctly to provide useful results.
2) Water-delivery schemes were quite different 85 years ago and not as well recorded. Most of the hydraulic structures that control canal flows in the recent simulation were not yet or only in the process of being built in the hindcast period.
3) The recent simulation is parameterized with modern high-resolution observed data and information. However, for the hindcast simulation, there were less observed data with greater uncertainty, requiring the use of modern surrogate data or synthesis of comparable data based on assumed differences between past and present conditions.
4) Representation of major storms with a spatially uniform wind field has been considered adequate for the recent simulation, as there was not a major onshore hurricane event during that interval. A storm in the hindcast simulation, such as the Great Miami Hurricane of 1926, however, involves a strong wind field with high-spatial variability and requires an accommodation to properly represent the wind forcing.
5) Due to the proximity of offshore boundaries in both TIME and BISCAYNE, the model cannot represent the long offshore fetch over which high-wind forces on the ocean surface pile up water against shorelines, producing a storm surge. It is therefore necessary to indirectly represent the effects of the surge at the model boundary. The water level or velocity can be specified at the boundary to induce the proper surge height or surge momentum.
6) The proper temporal scale for the representation of a major storm event is shorter than the 4-h averaged period used for the spatially uniform wind. The center of a hurricane traveling 20 km/h moves 80 km between 4-h time steps, a major portion of

the combined TIME/BISCAYNE domain. The model must be capable of resolving finer time steps for the storm event duration and represent the longer time steps for the rest of the simulation.

7) The spatial resolution at which the hurricane processes are represented must be based on the response of the affected hydrologic system. A model depiction with high-spatial resolution of a forcing function may not yield any more information than a depiction with a lower resolution forcing function, because the dynamics of the hydrologic system have a spatial scale that controls the response.

Purpose and scope

This manuscript documents the development of a hindcast simulation from the TIME/BISCAYNE simulated period 1996 to 2004. The hindcast model simulates storm events for the period of 1926 to 1932 and addresses past sea level and limited hydrology and meteorology data. This time interval was designed to include the 1928 synoptic aerial photo coverage of the South Florida peninsula, which documented past vegetation distributions and surface-water configuration. The simulation opens the possibility of referencing historic and modern vegetation to hydrologic changes. The interval also includes landfall of the Great Miami Hurricane (#7) of 18 September 1926 while several other hurricanes impacted the region providing a range of storms for comparison and future analyses (Figure 2). Model development requires realistic hurricane wind and storm surge representations to the proper spatial and temporal scales. Results are presented from simulations utilizing various hurricane representations to assess efficiency of the storm representations in the hindcast model, as well as to verify and validate the hindcast application. The objective of the hindcast is not to precisely duplicate past conditions, but to represent short-term processes such as storm-induced wind, rain, and surge, along with long-term hydrological variations, that affect ecological processes and ecological response to changes in hydrology.

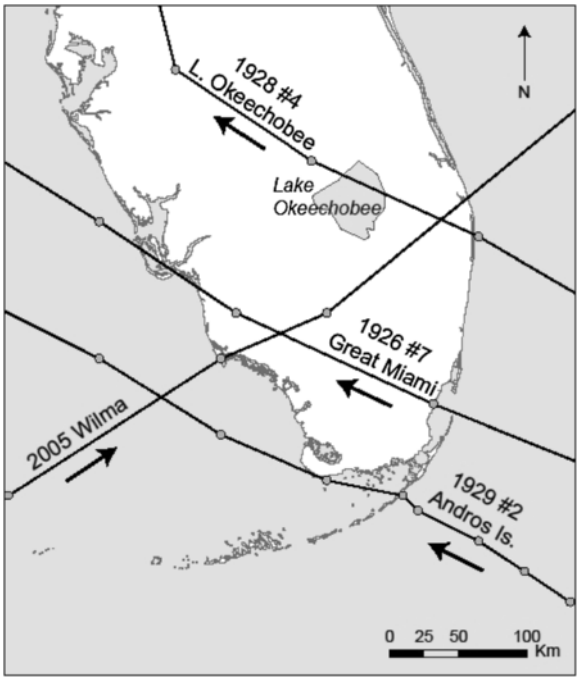

Figure 2 Selected hurricane tracks for South Florida. Figure compares hurricane tracks for the hindcast interval from 1926 to 1932 to the track of Hurricane Wilma in 2005. Storms from 1926 to 1932 were not given official names but numbers. Names provided are names of the storms commonly referred to in historical accounts.

Methods

Hindcast water-control structures

The 1926 to 1932 canal network was significantly less developed than in the 1996 to 2004 period. The only primary canals in place were the Tamiami Canal, Miami Canal, and Snapper Creek Canal along with several shorter coastal canals further south (Renken et al. 2005) (Figure 3). Modern canals were removed from the hindcast simulation by eliminating their leakage connection to groundwater and the associated regulated surface-water outflows. The hydraulic structures built on the primary canals after 1932 also were removed from the hindcast simulation, changing discharges from the coastal structures on Miami Canal and Snapper Creek Canal, S-26 and S-22, respectively. Modern flows are regulated for supply and flood control and, consequently, can be more sporadic and temporally variable than the past unregulated system. One representation of unregulated flows was to distribute the net recorded flows at each coastal canal outflow point as a constant value through the simulation period (Lohmann et al. 2012). With no data available for 1926 to 1932, mean flowrates for 1996 to 2004 were used as surrogates.

Hindcast topography

The modifications in topography for the 1926 to 1932 simulation are predominantly along the eastern coast (Figure 3) and primarily reflect the resetting of coastal elevations near modern canals to pre-development values. With minimal historic data, no alterations were attempted in the western TIME area, but the elevations near coastal canals were altered to match the adjacent cell elevations. The same leveling process was applied to the site of modern Turkey Point nuclear plant.

Hindcast surface-water inflows and tidal levels

The estimation of flows across the northern model boundary of the Tamiami Canal for the hindcast was accomplished through the construction of an empirical

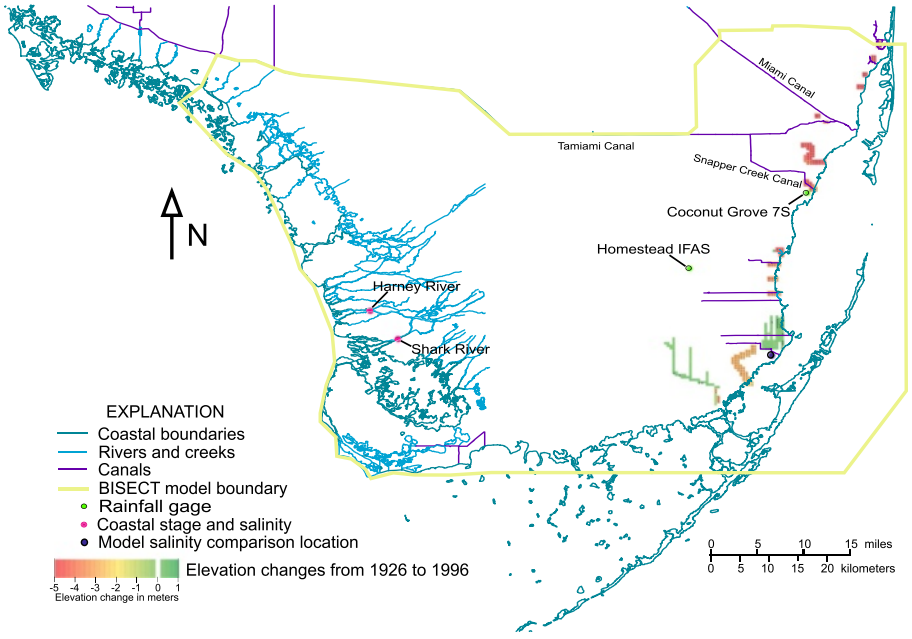

Figure 3 Study area in South Florida showing the parameters for the hindcast. Study area in South Florida showing model boundary, historic canal distribution, locations of historic topographic changes, and other parameters for the hindcast. Parameters include rainfall stations, surface features, wind field grid, and comparison locations for model results. Rainfall data were accessed from the DBHydro database provided by the South Florida Water Management District: (http://www.sfwmd.gov/dbhydroplsql/show_dbkey_info.main_menu).

relationship between recent flow and Lake Okeechobee (location in Figure 1) water levels. Although there have been a number of changes to the system over the years, the recent relation was used to estimate historic flow from historic water levels recorded back to the year 1912. Details of the empirical equation's development are discussed in Appendix 1.

Tidal water levels at the remaining boundaries were lowered from the 1996 to 2004 levels to values indicative of the 1926 to 1932 period based on a regression of historical water levels at the Key West Tidal Station, which has continuous record back to the year 1913 and sporadic measurements back to 1846 (Maul and Martin 1993). Tidal data indicate the mean sea level rose at the rate of 2.4 mm/year from 1933 to 2004, a total of 172.8 mm. The mean tidal levels computed for 1926 and 1932 are −0.390- and −0.373-m NAVD88, respectively, based on a −0.20-m mean level for 2004.

Historic groundwater conditions are poorly documented and insufficient information exists to define time-variant groundwater levels. The groundwater boundaries along the coastal areas are controlled by the overlying tidal levels and therefore change with the defined sea level. The Miami River was uncontrolled during the hindcast period and probably drained the area around it more than during the recent period. However, overall drainage through the region increased over time, so it is difficult to generalize the overall change to groundwater levels.

Data for daily parameters with no historical measures

As hydrologic information from this period is limited, the hindcast simulation utilized data from the 1996 to 2004 simulation as a surrogate for the unknown quantities, under the assumption that these time series were at least similar to values in the 1926 to 1932 period and no other assumed values were considered better. This modern time series includes parameters used to compute heat transport and evapotranspiration (ET) (solar radiation, relative humidity, air temperature), the wind field (with a modification discussed below), groundwater-level boundaries, offshore salinities, and tidal water-level fluctuations. A lower sea level in 1926 might mean that groundwater levels are lower inland as well, but the lack of drainage could mean a higher level. Groundwater levels at the coast are more controlled by sea level.

Hindcast long-term rainfall

Compared to the 107 rainfall gages available for the 1996 to 2004 recent simulation, only a few gages had been constructed by the 1926 to 1932 hindcast period. Rainfall values were averaged from the Coconut Grove 7S Station (Station # 06168) and the Homestead IFAS Station (Station #HB872) shown in Figure 3, referenced through the South Florida Water Management District DBHydro database (http://www.sfwmd.gov/dbhydroplsql/show_dbkey_info.main_menu).

Comparison of daily rainfall between the gages showed data were recorded throughout the 1926 to 1932 period. At least one station was in operation at all times, with the exception of the Great Miami Hurricane aftermath, when both stations were destroyed. In general, these stations provided a consistent measure of precipitation for the area. However, on several occasions, the gages provided substantially different measurements, likely related to the distribution and path of the storms across the model domain. For example, a storm on 7 September 1927 showed rainfall values of 4.1 and 0.39 in., for the Coconut Grove and Homestead gages, respectively. This type of observational difference, known as a correlation distance effect (Székely et al. 2007), is inherent to the limited spatial sampling of historical data. In general, the longer the averaging timescales, the more uniform the spatial distribution of rainfall, so monthly and yearly average tend to be more consistent between rainfall gages.

To assess the adequacy of using only two gages to represent past conditions, the data were input into the initial hindcast model and inundation output was mapped and examined on a daily time step to identify sudden inundation signatures indicative of a major rain event. The timing of each event was compared to newspaper and publication reports of past tropical storms. Inundation signatures corresponded with dates of the known major hurricanes in HURDAT, the official National Oceanic and Atmospheric Administration hurricane database (Landsea et al. 2008). Furthermore, the verification process identified major rain events not associated with tropical storms. The most notable was described as the 'Florida Disturbance' 27 May to 19 June 1930 (Fish, 1930). It is still one of the largest rainfall events ever recorded in the Miami area when 33.16 in. fell over the 24-day period. Although not associated with major winds and storm surge, such precipitation events can impact terrestrial and perhaps some marine species.

Missing rainfall during the 1926 Great Miami Hurricane

A major break in the rainfall data occurred when the rain gages were inoperable for 59 days following landfall of the 1926 Great Miami Hurricane. Two different methods to estimate the missing rainfall are discussed below: one based on historic estimates of barometric pressure extrapolated to rainfall, the other based on the forward speed of the storm. Mitchell (1926) reported that from midnight to 6:45 am on 18 September 1926, when the eye came ashore, rainfall was recorded at 0.28 in./h. However, a substantial portion of any hurricane's rainfall occurs in its tail, during which there were no measurements. Barometric pressure recorded from Miami at midnight was 29.5 mb but did not rise back to this level until about 6:00 pm (Mitchell 1926). If 18 h represents the period of rainfall, and the rate is assumed to be 0.28 in./h, then a total rainfall of 5.04 in. was estimated.

The alternative method developed by R. H. Kraft (Pfost 2000) is an empirical relationship, 100 divided by the forward speed of the hurricane (knots), which, for modern storms, provides a reasonable estimate of the resulting rainfall amount in inches. One example is Hurricane Andrew, which traveled at about 16 knots and dropped about 7 in. of rain; the Kraft method yielded an estimate of 6.25 in. The Great Miami Hurricane was estimated to travel at 18.75 mile/h (16.3 knots) as it approached Miami and 11.5 mile/h (10.0 knots) after hitting land (Mitchell 1926). This method yields estimates of 6.1 and 10.0 in. of rain from the storm, respectively, with probably more weighting to the lower value, which corresponds to landfall. Considering the previous estimate extrapolated from Mitchell (1926) of 5 in., a 6-in. total rainfall (0.152 m) was input into the simulation for 18 September 1926 as estimated rainfall from the Great Miami Hurricane.

Modeling storm surge

The method used to approximate storm surge requires modifying the boundary sea level conditions to represent water accumulated from hurricane winds offshore outside the model domain. When approximating surge for a specific hurricane in the recent simulation, the boundary stage conditions were iteratively modified until the simulated stage at coastal river outlets matched measured values.

Storm surge estimates for the Great Miami Hurricane were based on information from Mitchell (1926). Tidal water levels were set to values indicative of the hindcast period as discussed previously. The maximum storm surge height was recorded as approximately 8 ft (2.4 m) on the Miami side of Biscayne Bay and also at Miami Beach (Mitchell, 1926). The datum was not specifically defined, so it is assumed to be approximately defined relative to sea level at the time of the storm. These storm surge data were incorporated into the simulated tidal level with linear rises and falls occurring over a 6-h period consistent with the standard time step of weather prediction models (Landsea et al. 2012).

Storm wind field representations

In the computation of surface-water flow, wind speed is converted to force τ at the water surface in the momentum flux formula:

$$\tau = \theta \rho_{\text{air}} v^2$$

where ρ_{air} is the air density, v is the wind velocity vector at 10 m above the surface, and using a drag coefficient $\theta = 0.0018$. This is a nominal value used in previous applications (Wang et al., 2007). Using this relationship,

several methods of representing storm wind fields were developed for the hindcast simulation. The spatially uniform wind field defined for the daily simulation can be redefined to better represent large storms, or a spatially variable wind field at a shorter time step based on real wind data from an actual storm can be specified for the duration of the storm. The spatial resolution of the wind field can also be changed to determine the effects on the hydrologic simulation. These methods were compared and contrasted to determine the scale effects of wind fields on hydrologic response.

Spatially uniform wind fields

The peak velocity and storm duration recorded by Mitchell (1926) were used to make a spatially uniform storm wind field for the Great Miami Hurricane. The documented wind velocity increased to a peak of 56 m/s (125 mile/h) over 5-h period and dropped back to nominal velocities over the next 15 h. This time series was delineated as close as possible within the 4-h intervals of the uniform wind field developed for the recent simulation.

Spatially variable wind fields

As hurricanes have high-spatial variability in wind speed and direction as they cross land, a spatially variable dataset should improve the ability to simulate these storms events. A historic reconstruction for the Great Miami Hurricane (Landsea et al. 2012) was considered, but not used, as only the wind at the location of the hurricane's eye is reported every 6 h. Instead, an approximation was developed for a modern-era hurricane utilizing data from the 2005 Hurricane Wilma H*Wind Gridded Surface Wind Analysis (Powell et al. 1998), which is a data compilation based primarily on actual observations at sea, on land, from satellites, and from Hurricane Hunter aircraft. Past numerical simulations of storm surge have used wind fields created on the basis of fitting analytical cyclone models (Holland, 1980) or on surface wind field observations from H*Wind analyses of real storms (Zhang et al. 2008, Zhang et al. 2012). Real wind analyses provided more realistic wind velocity input for models, and storm surge output driven by these wind fields was compared with field measurements (Zhang et al. 2008, Zhang et al. 2012) for validation. No modern hurricane faithfully tracked the Great Miami Hurricane; however, Hurricane Wilma in 2005 was similar in spatial scale, and its track across South Florida from southwest to northeast can be compared to that of the Great Miami Hurricane from southeast to northwest when location and wind direction are switched from east to west (Figure 2). Using a real storm wind analysis from the study area provided the opportunity to compare different wind representations in the recent simulation to actual hydrology measurements in the field. Comparing output from the same storm run in both the recent and hindcast simulations allowed assessment of the efficacy of modifications to the recent model to produce a hindcast. Furthermore, using a modern storm provided experience with developing a diversity of known-storm scenarios that could be useful simulations for research and management questions.

The process to develop a variable wind field for the Great Miami Hurricane began with downloading the gridded H*Wind data posted for Hurricane Wilma. The wind data are presented as gridded values over an 8° × 8° area centered on the eye of the storm. There are 160 × 160 grid points for the entire area for a spacing of approximately 5.1 km (Figure 4). The TIME and BISCAYNE domains cover about 2% of the entire H*Wind grid, and values from the 5.1-km gridded data were spatially interpolated to the center of each of the 0.5-km grid cells. For Wilma, wind data were available at hourly intervals from 10:30 UTC to 16:30 UTC on 24 October 2005. Only the 7 hourly measurements were used for the analysis. Data values utilized include the location of the gridded wind measurement and the wind speed and direction.

The wind variable presented in the H*Wind data set is the maximum sustained wind speed over a 1-min average, the standard for hurricane wind measurements (Powell et al. 1996). The wind data are initially gathered at a 10-min average measurement but then multiplied by a gust factor to approximate the 1-min standard. The factor increases the value of the 10-min average velocity by approximately 11%. Because the minimum interval for the TIME/BISCAYNE simulations is also a 10-min average, this gust factor was removed by division of the output data values by the standardized gust factor of 1.11 (Powell et al. 1996).

In addition to the full resolution wind field described above, a reduced resolution representation was also developed to provide smaller data volume and computational effort for the hindcast. Whereas the full resolution grid bilinearly interpolates the wind data to the 0.5-km TIME/BISCAYNE grid, the reduced resolution grid divided the simulation area equally into a 4 × 4 grid (Figure 4) for a grid cell spacing of approximately 32 km in the east-west direction and 24 km in the north-south direction. The 16 cells formed a 4 × 4 matrix of spatially variable wind values that changed with each of the 7 hourly measurement from the Hurricane Wilma H*Wind analysis during the passage of the storm. Thus, the increase in area and reduction in resolution of each grid cell is approximately 30×.

In order to synthesize a spatially variable wind field surrogate for the Great Miami Hurricane, it was noted that the track of Hurricane Wilma from southwest to northeast is reflective of the Great Miami Hurricane from southeast to northwest (Figure 2) when location

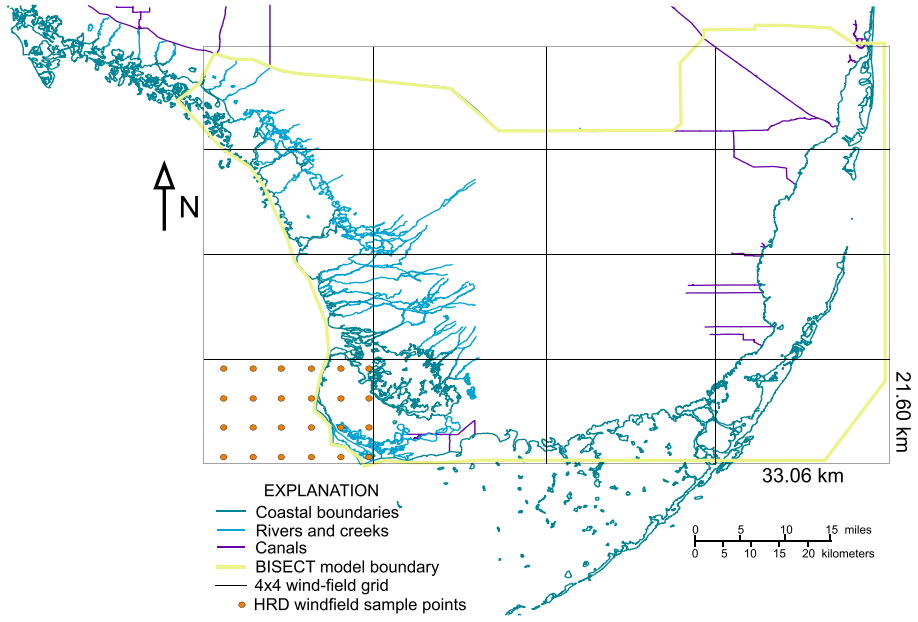

Figure 4 Reduced 4 × 4 TIME/BISCAYNE wind grid showing relation to original full resolution H*Wind sample points for Hurricane Wilma.

and wind direction are switched from east to west. The 4 × 4 variable wind grid from Wilma (Figure 4) was transformed in a similar manner, and the resulting wind field represented a storm traveling from southeast to northwest like the Great Miami Hurricane. The transformed time series of wind data from Wilma was scaled in wind speed magnitude and used as a spatially variable surrogate for the Great Miami Hurricane wind field. The peak wind speeds for the Wilma data are approximately 45 m/s (100 mile/h) whereas the peak winds reported for the Great Miami Hurricane were on the order of 56 m/s (125 mile/h) (Mitchell, 1926), so the wind speed data were all multiplied by a factor of 1.25 to approximate the Great Miami Hurricane wind field.

Short-term storm representation in long-term simulation

The spatially variable wind is defined on a shorter time step (1 h) than the default longer-term spatially uniform wind (4 h). In order to accommodate transitions between these two timescales, the FTLOADDS model code was modified to accept a separate gridded data set for the duration of the storm and use the standard time series of uniform wind for the rest of the time. Negative time step values indicate use of gridded data for storms. The ratio of the wind grid size to the model grid size is specified in the main surface-water input data set (Swain, 2005). Not only can this input format be used to represent a single storm, but the wind data set can be flagged at any time during the simulation and the subsequent array of wind in the gridded wind set will be used.

Verification and validation of the new components models

TIME/BISCAYNE has been tested thoroughly and calibrated for the recent 1996 to 2004 period by comparison to measured field data (Swain and Lohmann, US Geological Survey, March 2014, written communication). Much of the hindcast 1926 to 1932 simulation input is based, by necessity, on spatial information used in the calibrated recent model. However, the available historic field data for sea level, tidal level, rainfall, and surface-water inflows, although limited, are major drivers of key hydrologic processes. With reasonable depictions of past water control features and more realistic representations of wind fields and storm surge for landfall hurricanes, differences in hydrologic parameters that affect ecological response, such as salinity and percent time inundated, should be apparent in comparisons of output from the hindcast and recent models and should be consistent with expectations from known hydrologic principles and historic observations. Verification and validation of the efficiency of the hindcast modifications can be assessed based on differences between models and not between model output and observations. Furthermore, the time periods and storm events depicted in the simulations were also designed to provide insight into how the variability of hydrologic conditions can affect flow and salinity regimes in coastal surface waters and groundwater. Comparisons of these simulations yield information not possible without numerical modeling.

Model simulations

The various storm representations were incorporated into both the recent 1996 to 2004 and hindcast 1926 to

1932 simulations to compare and contrast their efficacy in modeling hydrological processes. Table 1 outlines the model simulation scenarios, their parameterization, and the acronym to identify each simulation. The varieties of conditions described in Table 1 lend insight into the effects of the storms, their parameterization, and the other hydrologic conditions that affect the storm's impact.

Simulation sets for the recent period

Simulations of the recent period were needed to examine the effects of a representative modern storm and the efficiency of a reduced wind field representation to approximate a known storm. The original 1996 to 2004 simulation provides a reasonable time series, but does not contain an appropriate modern storm with sufficient hydrologic measurements. Instead, wind, rain, and storm surge representations for Hurricane Wilma, which struck the Everglades on 24 October 2005, were synthetically inserted on 18 September 1996. This is 262 days into the recent simulation, the same point as the 1926 Great Miami Hurricane strike in the hindcast simulation, with a sufficient period following the storm to examine long-term processes such as groundwater and surface-water salinity effects. Rainfall data collected at the modern stations when Hurricane Wilma struck the study area were used to represent storm precipitation. The storm-surge-height time series was obtained from data collected at the Harney River and Shark River sites (Figure 3) during the actual storm.

Three wind field scenarios were simulated in the recent experimental set (Table 1):

1) with the 4 × 4 reduced wind data for Hurricane Wilma (Simulation RWVL);
2) the full wind data grid for Wilma, which is on a 5.1-km spacing (Simulation RWVH); and
3) the 'base' simulation, which included no spatially variable wind, only the uniform wind from the original daily time step (Simulation RN).

Table 1 Simulation runs, time periods, and storm configurations

Simulation run	Time period	Storm simulated	Wind field grid used
RN	Recent	none	none (TIME/BISCAYNE daily wind only)
RWVL	Recent	Wilma	Spatially variable, low resolution
RWVH	Recent	Wilma	Spatially variable, high resolution
HWVL	Hindcast	Wilma	Spatially variable, low resolution
HN	Hindcast	none	none (TIME/BISCAYNE daily wind only)
HGU	Hindcast	Great Miami	Spatially uniform
HGVL	Hindcast	Great Miami	Spatially variable, low resolution rotated

Each simulation is identified by its acronym describing the time period (R = recent or H = hindcast), the name of the storm represented (W = Wilma, G = Great Miami, or N = none), the type of wind field (U = spatially uniform or V = spatially variable), and the resolution of the wind field (L = low or H = high).

Comparison of the three simulations provides information on how much spatial resolution is needed to represent the wind effects on hydrology. The simulations also provide a validation of the wind field and storm surge used in the hydrodynamic models when salinity- and stage- simulated output is compared to empirical data collected during and after Hurricane Wilma.

Simulation sets for the hindcast period

Four simulations were run in the hindcast experimental set (Table 1):

1) with no simulated wind field for the storm (Simulation HN),
2) the surrogate Great Miami Hurricane with spatially uniform wind field (Simulation HGU),
3) the surrogate Great Miami Hurricane with low-resolution spatially variable wind field (Simulation HGVL), and
4) the modern Wilma low-resolution spatially variable wind field (Simulation HWVL).

The comparison of the first three simulations indicates effects based on three representations of the wind field. Including a modern storm in the hindcast period (Simulation HWVL) allows a comparison of the same storm in the two time periods, yielding some insight into the importance of various ambient hydrologic conditions on the response to a particular storm event. Furthermore, the insertion of these major storms at the beginning of the recent and hindcast simulations provides a 7-year period to examine long-term effects to surface-water and groundwater hydrology that is not yet available for any recent, naturally occurring major hurricane in the region.

Results and discussion

Simulations in the recent period (1996 to 2004)

Calibration of Wilma storm surge values to empirical measurements. [Runs RWVL and RWVH]

For the recent simulation interval, which included a Hurricane Wilma-type storm (RWVL and RWVH, Table 1), model boundary sea level values were calibrated to measured inland storm surge values for the Shark and Harney Rivers during and following Hurricane Wilma. A Wilma storm-surge height time series was obtained by averaging data collected at the Harney River and Shark River sites (Figure 3) for a 56-h period starting 16 September 1996

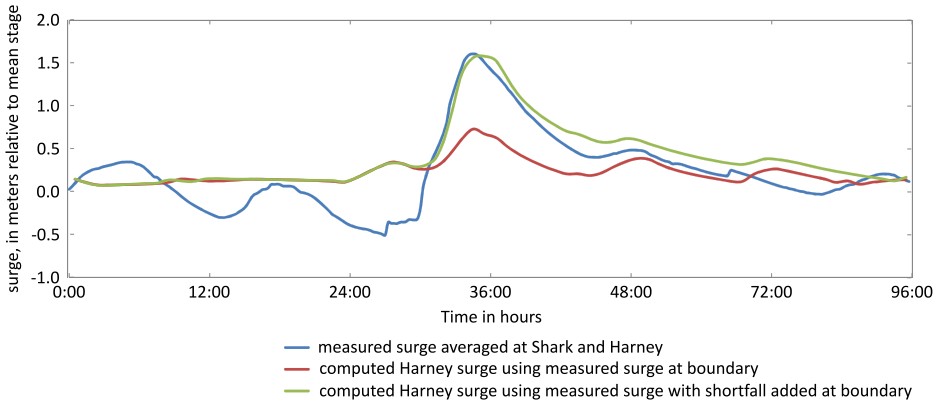

Figure 5 Measured (blue line) and model computed (red and green lines) surge heights.

(blue line Figure 5). These tidal levels for the storm surge were applied at the western boundary of the recent simulation with the reduced 4 × 4 wind grid (Simulation RWVL, Table 1). Due to wave-energy dissipation between the boundary and coastline, initial surge heights computed at Harney River, shown by the red line (Figure 5), were too small. An iterative process was used to raise the peak boundary surge levels until the modeled response at the two stations matched the measured levels during Wilma. The difference between the measured stage and the simulated stage at Harney was added as a correction to the boundary stage and re-simulated. The new stage (green line, Figure 5) is a much better match to the measured stage and was used to represent a synthetic Wilma storm surge in the hindcast simulation.

Effects of different wind field grid resolution [Runs RWVL and RWVH]

Both the original full H*Wind grid resolution and the 4 × 4 wind grid for Hurricane Wilma were superimposed on the 1996 to 2004 recent simulation interval on 18 September 1996, the same day of the year as when the Great Miami Hurricane made landfall in South Florida (Table 1 simulations RWVL vs. RWVH). Comparisons between these two model results for salinity averaged for this day (Figure 6) show that the inundation and surface-water salinity distributions after the hurricane are nearly identical in spite of the large difference in resolution of the input wind. There is a difference of several square kilometers in the small dry areas in the northwest area of the model in the midst of the freshwater inundation area, but otherwise, the model run results are nearly identical. These results imply that reduced wind field resolution can be effectively used in representing wind fields in hindcast applications.

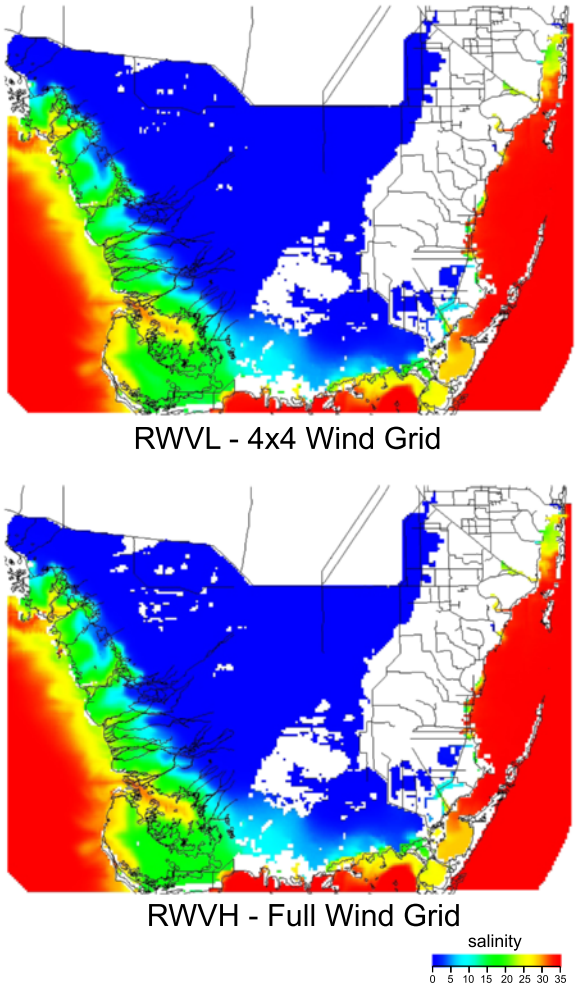

Figure 6 Inundation and salinity simulated 18 September 1996, induced by synthetic Wilma-type storm with differing wind resolution. Uncolored areas are not inundated.

Verification of efficiency of the Wilma storm representation [Runs RWVL and RWVH]

The recent simulation allows verification of the hydrodynamic model storm representation by comparing surface-water salinity values recorded at the gaging stations during Hurricane Wilma on 24 October 2005 to results simulated for the same locations from the synthetic Wilma storm on 18 September 1996. Salinity values are shown in Figure 7 for a 72-h interval encompassing the landfall of Hurricane Wilma. Data for two gaging stations were used for comparison: one at the Harney River and the second at the Shark River (Figure 7). The pre-hurricane salinities were higher in the simulated period (1996) compared to the measured data (2005). Despite the different pre-hurricane conditions, the storm processes were so dominant that post-storm observed and simulated results were similar; measured/computed differences pre- and post-surge of 3.76 PSU before and 1.40 PSU after for Harney River and 8.25 PSU before and 2.40 PSU after for Shark River (Figure 7). Furthermore, the period of salinity rise and fall was identical for both the full wind grid RWVH and the reduced 4 × 4 wind grid RWVL. This finding further supports the previous result that simulating variable winds with differing wind resolutions does not seem to produce substantially different results. Coastal flows appear to be more heavily influenced by general wind direction and storm surge rather than small-scale wind variations.

Hindcast simulations

Efficacy of surrogate variable wind field for the Great Miami Hurricane [Run HGVL]

Results described above demonstrate the validity of the storm simulation in the recent environment (1996 to 2004), setting the stage for representing the Great Miami Hurricane in 1926 through the insertion of a surrogate hurricane wind field. The hypothesis was that a transformed time series of wind data from Wilma could be scaled in wind magnitude and used as a spatially variable surrogate for the Great Miami Hurricane wind field, capturing storm processes salient to known hydrological response.

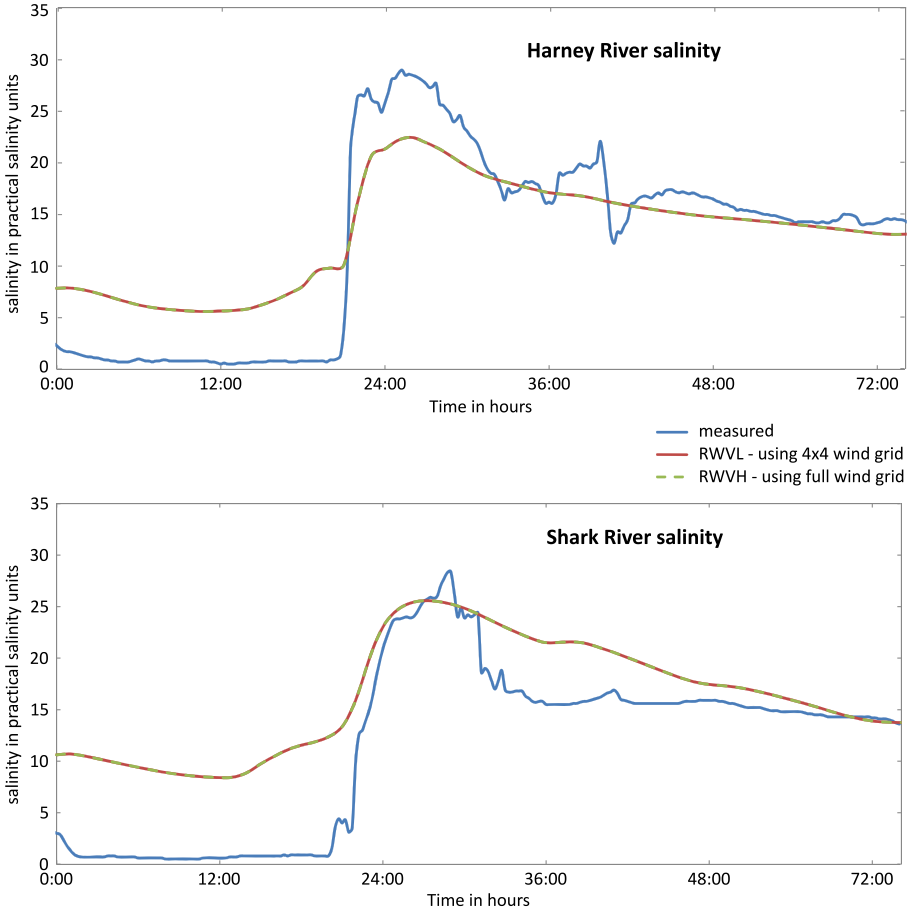

Figure 7 Measured salinity at Harney and Shark Rivers and simulated values with differing wind schemes, RWVH and RWVL.

The approximated historic wind field of the 1926 storm using the 4 × 4 reduced resolution wind field (Simulation HGVL) at hourly intervals (Figure 8) clearly delineates the eye of the hurricane at hour 2, and the hurricane has largely passed by hour 3. One key directional component was changed in this simulation: the storm tracked from southwest to northeast in the 4 × 4 grid for Hurricane Wilma but was rotated about its north-south axis to correspond with the Great Miami Hurricane storm, which tracked from southeast to northwest. In this transformed dataset, the maximum winds move from the coastal areas of Biscayne Bay through the Everglades northwesterly. Three hours later, the storm center moved almost entirely outside the northwestern boundary of the simulation area (Figure 8). The change was rapid within the first 3 h so that the areas of highest winds along the southeastern model area had some of the lowest winds by the third hour after landfall.

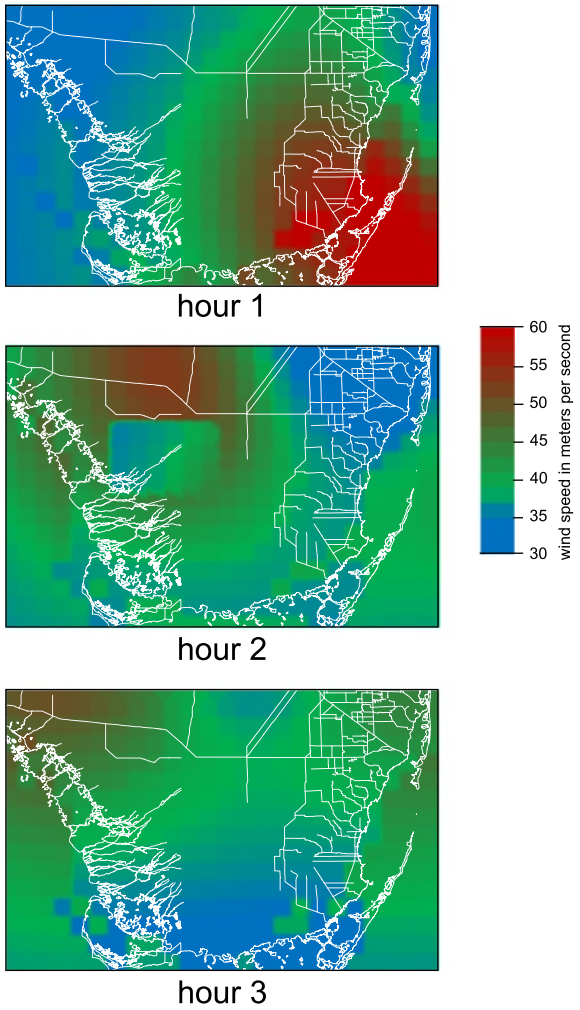

Figure 8 Wind fields synthesized for Great Miami Hurricane 1926.

Effect of different wind field grid resolutions on hydrological response [Runs HGU, HGVL, and HN]

The hindcast period was simulated with three different representations of wind for the 16-h period on 18 September 1926 during the Great Miami Hurricane, described as HGU, HGVL, and HN above. All input parameters for the first two simulations are identical, including storm surge and rainfall, with the exception of the wind field on the day of the hurricane strike. The third simulation does not have the simulated storm surge and storm rainfall, so all hurricane-related phenomena are absent from HN.

Simulated surface-water salinity values were compared immediately preceding the storm, the day of landfall, and then several months later for a subset of the model area west of Biscayne Bay where the storm came ashore (Figure 9). Surface-water salinity the day before the hurricane, 17 September 1926, is identical in the three simulations, but at the end of the following day, salinity intrusion from storm surge simulated in HGU and HGVL is clearly higher than in HN (Figure 9). Similarly, the overall freshwater inundation area is larger when the hurricane is simulated, as would be expected from the rainfall rate. The salinity values in the southeastern coastal area are particularly affected by the simulated Great Miami Hurricane as shown in the Figure 9 comparisons. Florida Bay and southern Biscayne Bay are less saline in the two hurricane simulations, primarily because of the storm-related rainfall. Comparison of inundation and salinity for September 18 from simulations HGU and HGVL indicate higher values with the spatially uniform wind field (HGU), which has winds coming from due east for the entire model area. With the counterclockwise rotation of the storm, the spatially variable wind on the southern side of the storm comes from the west, so the uniform wind representation is obviously wrong in this area and the inundation too high (Figure 9 HGU). The difference is seen after 1 month (18 October 1926) where the spatially uniform wind simulation HGU has 1.25 km^2 more inundation than HGVL with spatially variable wind. Consequently, the spatially variable wind field produces a representation compatible with the counterclockwise pattern of the hurricane winds.

As expected, simulations without any hurricane wind field (HN) show almost no change in salinity and inundation during the days immediately around landfall. One month later on October 18, substantial differences still exist due to the hurricane. Even after another month, on November 18, the differences in inundation and salinity are still noticeable, although the storm and no-storm simulations are starting to show similarity. An important consideration is that, over the 30 days following the Great Miami Hurricane of 1926, 6.2 in. (15.7 cm) of rain were measured. The equivalent 30-day period after

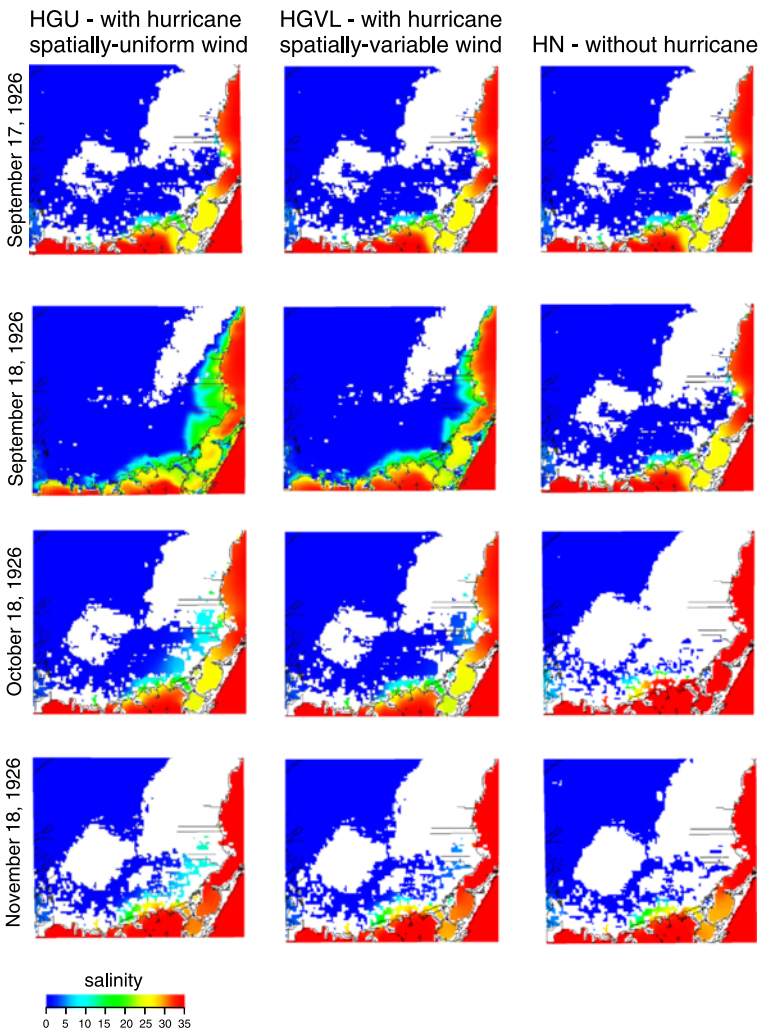

Figure 9 Salinity maps for hurricane and no-hurricane scenarios for the southeast quadrant of model (see Figure 3). Florida Bay and southern Biscayne Bay are on figure bottoms and bottom's right, respectively.

the Wilma-type surrogate storm in 1996 had 9.8 in. (24.9 cm) of rain. The drier conditions in 1926 allow the inundation and salinity affects to remain longer than if there had been additional rainfall.

Long-term effects of surface-water and groundwater salinities under three wind field scenarios [Runs HGVL and HN]

Besides comparing the areal distribution of salinities after the landfall of the Great Miami Hurricane under the different wind scenarios, the long-term salinity response was also examined. The long-term effects on surface-water and groundwater salinity are shown at a comparison site (model salinity comparison location, Figure 3) in the southeastern quadrant of the model. This onshore area consists of isolated small coastal wetlands, seasonally inundated, where minimal flushing is likely. Simulated surface-water and groundwater salinities at this location are compared for 6 years after the initial landfall of the Great Miami Hurricane in the HGVL simulation (Figure 10). The surface-water salinity is seen to peak early and drop off at a slowing rate for about 36 months. In contrast, the groundwater salinity in the first model layer, computed at a depth of about 1.25 m below land surface, shows a much longer delayed response, peaking at the end of the following dry season. While the lag is present in both the HN and HGVL wind scenarios, the variable wind scenario does not show the effect as strongly as the uniform wind case. Because the spatially variable wind field model provides a more realistic approximation of hurricane processes, it also most likely provides a better assessment of storm surge effects.

The implication from these simulations is that storm surge effects in the aquifer can last for years; however, there is some uncertainty in the actual length of time because numerical model predictions near this coastal area

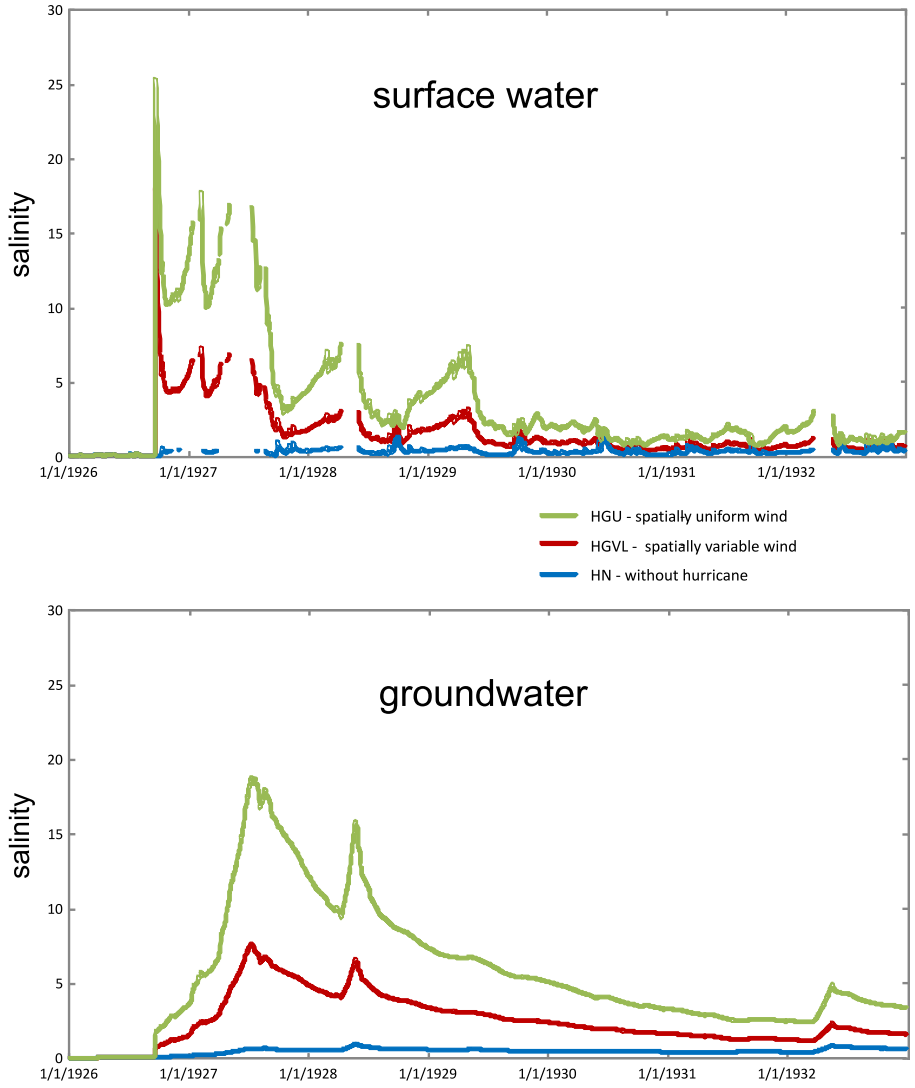

Figure 10 Salinities in surface water and groundwater predicted for scenarios. Breaks in the surface-water plots indicate times without inundation.

indicate a salinity accuracy of less than 3 PSU for most computed values (Lohmann et al. 2012). Observing when the difference between the salinity with and without the hurricane effects drops below this value (Figure 11) indicates, in certain areas, substantial surface-water effects for at least 2 years and groundwater effects are important for at least 3 years. Moreover, groundwater chloride data collected after Hurricane Andrew from well G-901, which is located slightly further north than the area discussed but still within coastal southeast Miami-Dade County, show a definite increase in salinity for at least 3 months after the 1992 storm and possibly extending out almost to 2 years (http://nwis.waterdata.usgs.gov/usa/nwis/qwdata/?site_no=254201080173001). The prolonged salinity effects are most likely due to the local topography providing minimal flushing.

Comparison of hindcast and recent simulations

Comparison of the overall hindcast and recent simulations [Runs HWVL and RN]

Mapping the percent of time, during the entire simulation, that each model cell is inundated provides a comparison of the basic characteristics of the two time periods. Substantial differences are seen in plots of percent-time inundated when comparing average daily values from the recent and hindcast intervals (Figure 12). Coastal areas are drier in the hindcast period due to the lower mean sea level, especially in the southwest. Even in the northernmost part of the model, areas are drier in the hindcast simulation, partially due to lower groundwater levels caused by the Miami Canal's uncontrolled drainage present in the hindcast period. However, it is interesting to note that the area just south of the Miami Canal is slightly wetter during the

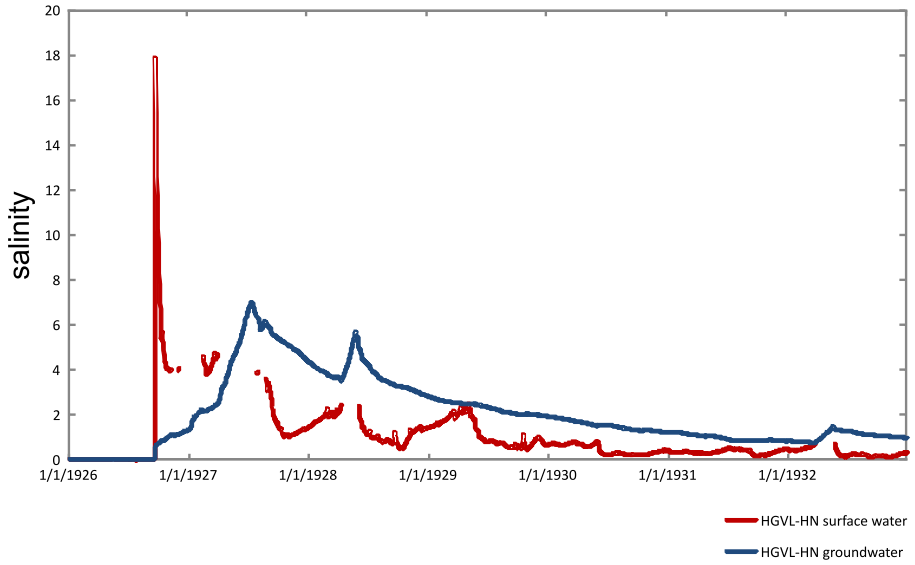

Figure 11 Salinity differences between hurricane and no-hurricane scenarios.

hindcast simulation due to the poorer flood control and fewer control canals at that time (Renken et al. 2005).

Effect of existing conditions and surface-water control features in hydrologic response to the same storm [Runs HWVL, RWVL, and RN]

The relative impact of a simulated storm event on the hindcast and recent scenarios can be illustrated by displaying inundation and salinity maps generated for the day following the insertion of a synthetic Hurricane Wilma (HWVL 19 September 1926 and RWVL 19 September 1996, Figure 13). The same storm winds are represented occurring in the two historical periods with differing hydrologic conditions. The distributions of salinity and inundation are the most similar between the two periods on the western coastal area where the storm came ashore; they become more dissimilar when observing further eastward. This dissimilarity is likely related to the more extensive surface-water control network in the east (Figure 13) during the recent period. Although pre-storm conditions and hydrological infrastructure (canals, topography) are substantially different between the two time periods, storm processes largely overcome those differences and the simulations converge in the storm inundation area. This comparison shows that the storm processes salient to hydrological response are captured in the model and appropriate to use in other storm scenarios. The third simulation in the recent period without the hurricane winds, surge, and precipitation (Simulation RN, Figure 13) shows surface-water inundation and salinity conditions if the storm had not occurred. Comparison with Simulation RWVL shows the effects of the hurricane are largely concentrated on the west coast where the storm came ashore.

Comparison of measured and simulated river salinity values for Wilma-type storm inserted into the recent and hindcast

Simulations HWVL and RWVL also provide comparisons of the simulated salinity values at Harney and Shark River sites (Figure 3) during the Wilma-type storm in the recent and hindcast periods (Figure 14). Little difference is seen, but at both locations, the hindcast storm salinity did not peak as high and took longer to wash out than the recent simulation. This observation might suggest more freshwater flow variability was recorded in the recent simulation, which can either be due to more details available in the data record of the recent simulations or that there was actually more variation in the recent interval.

Conclusions

The hindcast model demonstrated good capabilities of capturing long-term, large-scale hydrological processes while incorporating short-term processes inherent to hurricanes. Despite data input limitations and the lack of historic field measurements to validate the model, comparison of recent and hindcast period simulation experiments (summarized in Table 2) showed similarities and differences expected from known physical principles and empirical studies of past storms (Davis et al. 2004; Wilson et al. 2011). Development of surrogate wind fields from H*Wind analysis of direct observations of Hurricane Wilma provided realistic representations of storm effects and implies that simulations of historical hydrology can be reasonable in spite of the lower resolution data sets associated with historical eras. Output from running the surrogate representation at a shifted time frame in the recent and hindcast simulations showed values similar to field-measured data collected in real

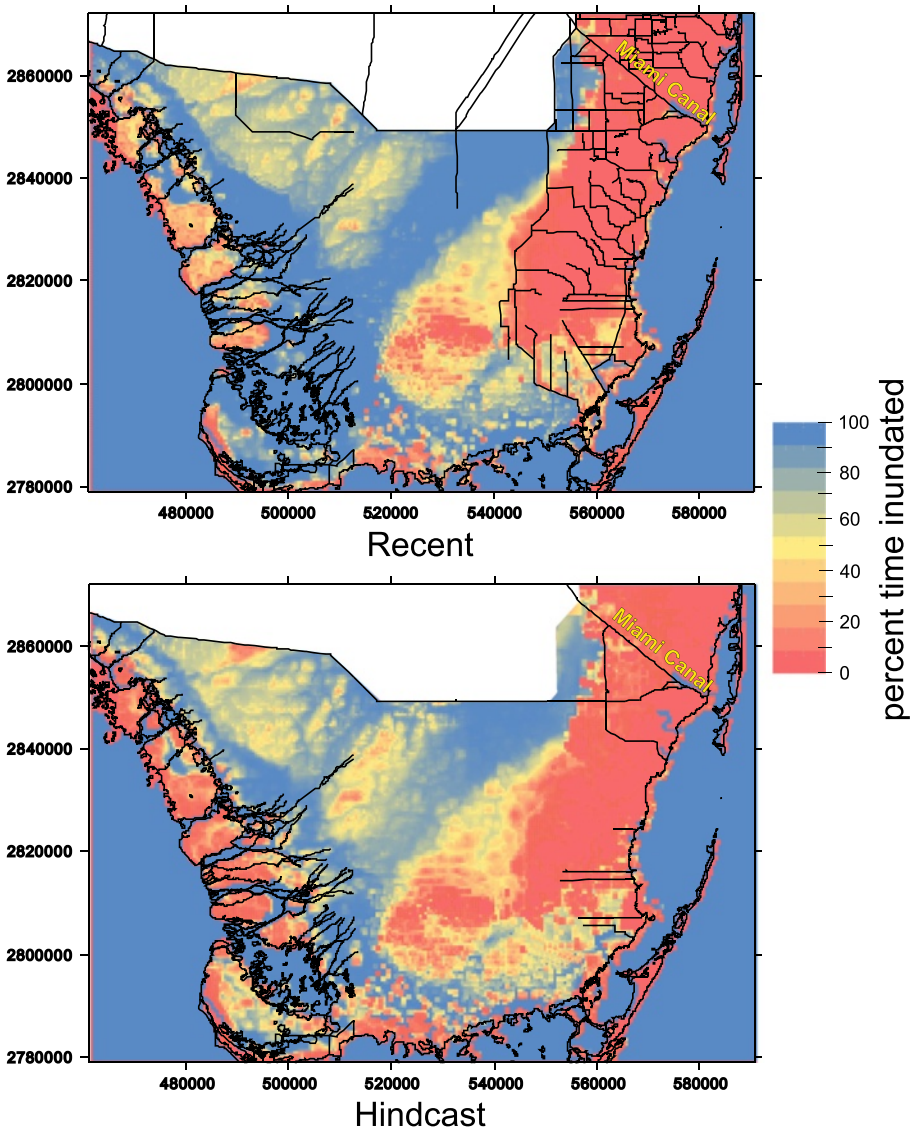

Figure 12 The percent of time inundated for the 1996 to 2004 simulation and the 1926 to 1932 simulation.

time. Inundation signals for rain storms in the hindcast based on 2 rain gages were similar to those in the recent based on 107 gages. These outcomes provide greater confidence that the approximations employed in the hindcast model are valid.

The hindcast model shows promise for use in ecological studies to test hypotheses based on theoretical- or empirical-based studies at larger landscapes and timescales. Processes on a wide range of timescales are represented by the simulations: surface-water flow at 10 min, wind at 1 to 4 h, rain at 6 h to 1 day, and groundwater flow at 1 day, with a multiyear simulation period amenable to the timescale of ecologic changes. With the strong dependence of coastal vegetation composition on salinity, results of the model comparison could provide useful input for a variety of ecological models. The information can be input to any relevant study or application as a difference in surface-water and groundwater salinity between the spatially variable wind hurricane scenario and the no-hurricane scenario. By identifying the salinity difference between model runs, errors in model mean values largely cancel out. This difference can be combined with field-derived information and applied to habitat models, vegetation succession models, and individually-based models to provide realistic storm-induced salinity related evaluations.

While the effects of hurricane wind fields on surface-water and groundwater salinity can have an inherent time lag of multiple months or years (Wilson et al. 2011), the effect on coastal vegetation is possibly much slower and of

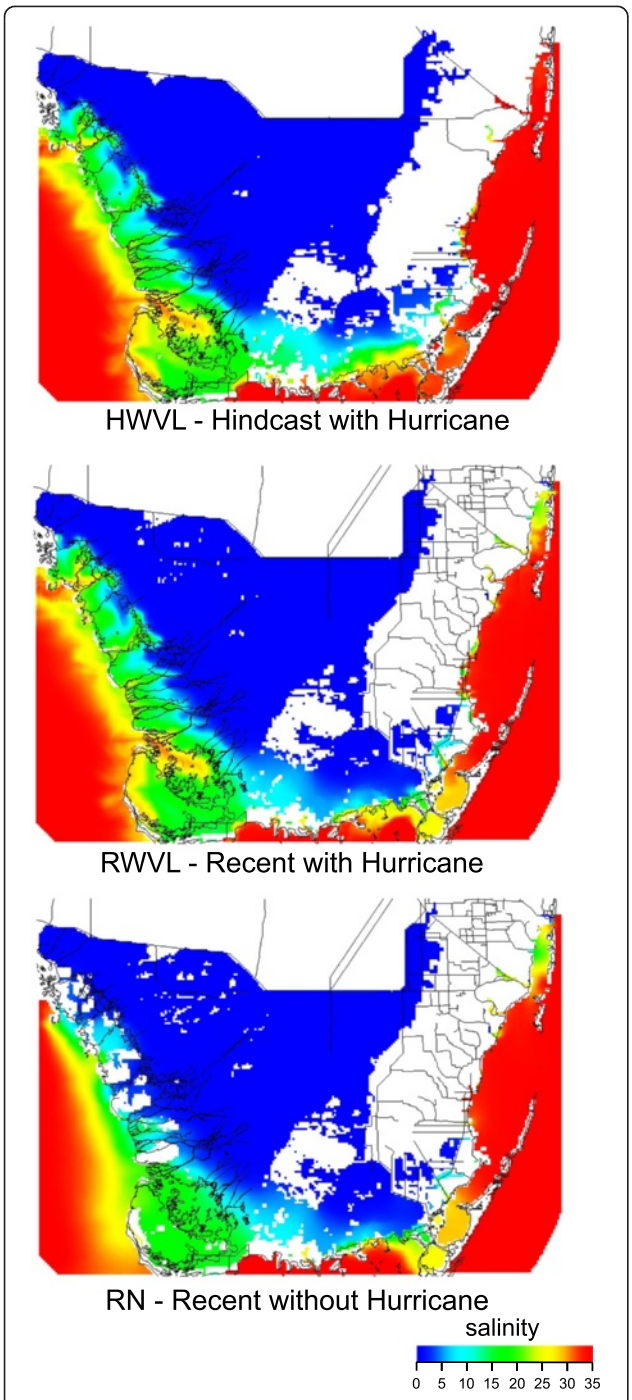

Figure 13 Inundation and salinity following Wilma-type storm in hindcast simulation and recent simulation (uncolored areas are not inundated).

longer duration. Saha et al. (2011) and Jiang et al. (2012) have shown that the population of mangroves and tropical hardwood hammocks can be substantially affected for decades after a salinity event. The balance between the two plant populations heavily depends on soil salinity. Clearly, individual, large storm events must be considered when determining the long-term change in coastal ecology. The results of this study demonstrate that a storm event may have effects on groundwater salinity extending for years, depending on location and *in situ* hydrology.

If hindcast studies integrating this numerical model with ecological models reliably show process and effects in the past, then these methods can be applied with more confidence in forecasting in areas of further research, which have even more data and resolution limitations. Any representation of rare events like hurricanes in a forecast will require generation of random events to represent a storm. Rather than be restricted to random presentations, we believe that users of the model would be better served if they can generate and modify various actual storm scenarios and apply it to a particular area of interest in a series of what-if questions. This is the technique we applied for representation of the missing wind field for the 1926 Great Miami Hurricane. While clearly, no two hurricane wind fields are the same, the simulation of a known storm provides some basis for comparison, given the approximations needed to make a hindcast, which are amplified when making a forecast. The insertion of a synthetic Hurricane Wilma shows the technique works with modern simulations with high-data resolution, giving us more confidence in the hindcast and forecast projections. Scenario planning (Peterson et al. 2003) has been embraced by the National Park Service as a tool to develop management plans under the uncertainty of future climate change (Weeks et al. 2011). Forecasting a range of plausible future conditions and disturbances allows managers to explore multiple strategies for water resource management in response to climate change.

Appendix 1 - development of empirical Lake Okeechobee/recent flow relationship to define hindcast model inflows

The empirical relationship to water levels in Lake Okeechobee included a superimposed sine function to represent the yearly wet-season/dry-season cycle of flows across the Tamiami Trail. The amplitude of the sine function at any time is a power function of the stage in Lake Okeechobee with the following empirical equation:

$$Q_{\text{trail}} = C\,(Z_{\text{lake}} - Z_{\text{min}})^{p}\,[\alpha + sin\,(\varphi + \omega t)] \quad (1)$$

where Q_{trail} = computed flow across the Tamiami Trail, C = constant multiplier to produce flows in m^3/sec, Z_{lake} = stage in Lake Okeechobee in feet NGVD29, Z_{min} = minimum stage in Lake Okeechobee in feet NGVD29 at zero flow, p = exponent for lake stage function, a = scale factor to define mean flow rate, φ = phase

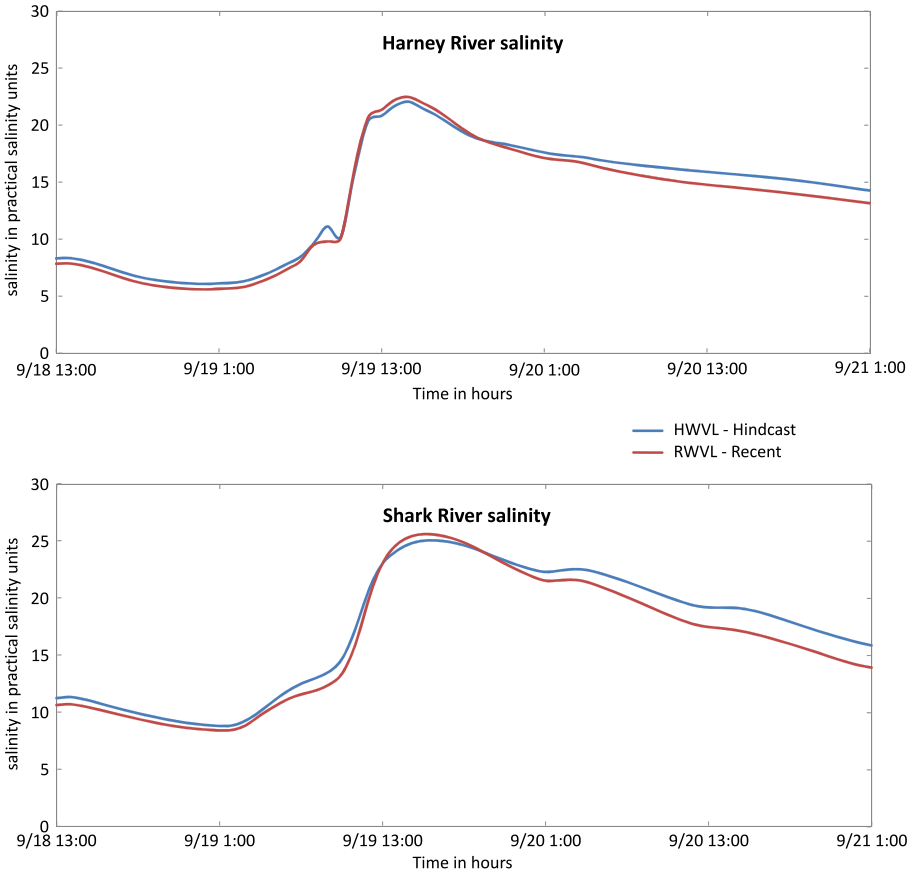

Figure 14 Comparison of Harney and Shark River salinity values for Wilma-type storm in hindcast simulation and recent simulation.

shift for sine function, ω = frequency of yearly flow fluctuation, and t is the time in days. The value of t is set with Day 1 being 1 January 1900, and the frequency of yearly flow fluctuations is fixed at $\omega = 2\pi$ radians/365.25 days = 0.0172/day. This ensures that the cycle of wet and dry season always is synchronized with the calendar. The variables C, $Z_{\min}$, p, a, and φ are determined with a Newton-Raphson solver using measured values of Z_{lake} and minimizing the difference between Q_{trail} and measured flows at the Tamiami Trail. This yields best-fit values of $C = 0.1076$ m^3/sec, $Zmin = 0.144$ m, $p = 4.29$, $a = 1.2245$, and $\varphi = 3.281$ radians.

Equation 1 is used to compute flows across the Tamiami Trail using the Lake Okeechobee stage, which is shown with the shorter period of measured flows in Additional file 1: Figure S1a. An expanded view of the period where measured flows exist is shown in Additional file 1: Figure S1b. This method reproduces measured flows with an explained variance of 58.7% expressed by the Nash-Sutcliffe coefficient. Additional file 2: Figure S2

Table 2 Comparisons of model simulations and conclusions

Simulations compared	Purpose of comparison	Conclusions
RWVH and RWVL	Effects of wind field grid resolution	Low resolution wind grid is sufficient to represent hurricanes, saving data and computational effort
HGU and HGVL	Effects of spatially uniform wind field grid and spatially variable wind field grid	The depiction of hurricane winds as uniform does not provide necessary storm wind geometry
HN, HGU, and HGVL	Effects of major storms on hydrology	Storms can have substantial long-term effects on groundwater salinity with consequences for vegetation
RWVL and HWVL	Effects of same storm in different time periods	Storm effects are quite similar for the same storm in different time periods
RN and HGVL	Hindcast and recent simulation general comparison	Historical changes in hydrology are primarily traceable to sea level variability and water-management changes

shows the cumulative volumes measured and computed by Equation 1. It tends to overestimate the total volume over the 1996 to 2004 period by only 18.6%, which is reasonable. Therefore, the computed time series shown in Additional file 1: Figure S1a is used as flow input at the northern boundary of the hindcast simulation. As there were no hydraulic structures at the hindcast simulation time, distributing the flow evenly across the northern boundary seems like a reasonable assumption.

Additional files

Additional file 1: Figure S1. Simulated Tamiami Trail flows 1917 to 2004 and Lake Okeechobee water levels. Figure S1a is the entire record from 1917 to 2004. Figure S1b is an expanded view of the recent simulation from 1996 to 2004 comparing measured to simulated flows.

Additional file 2: Figure S2. Cumulative measured and simulated Tamiami Trail flows from 1996 to 2004.

Abbreviations

HGU: hindcast time period with Great Miami Hurricane, spatially Uniform wind field; HGVL: hindcast time period with Great Miami Hurricane, spatially variable wind field at low resolution; HN: hindcast time period with no storm; HWVL: hindcast time period with Wilma storm, spatially variable wind field at low resolution; RN: recent time period with no storm; RWVH: recent time period with Wilma storm, spatially variable wind field at high resolution; RWVL: recent time period with Wilma storm, spatially variable wind field at low resolution; FTLOADDS: flow and transport in a linked overland/aquifer density-dependent system; SWIFT2D: surface-water integrated flow and transport in two dimensions; TIME: tides and inflows in mangroves of the everglades; H*Wind: Hurricane Wind Analysis System developed by the National Oceanic and Atmospheric Administration's (NOAA) Hurricane Research Division (HRD) (Powell et al. 1998).

Competing interests

The authors declare that they have no competing interests.

Authors' contributions

EDS developed and coded the numerical model modifications for the hindcast model and hurricane representations, analyzed the results, and drafted the initial manuscript. DK developed the concept of using a modern day wind field as a surrogate for historical hurricanes, collaborated with EDS to implement the wind field representations into the numerical model, validated the model inundation signal to historic hurricane and precipitation events, and wrote parts of the manuscript. CAL wrote parts of the manuscript and reviewed the manuscript from the perspective of facilitating communication of technical aspects to ecologists and resource managers. All of the authors contributed to the design of the simulation experiments, reviewed and revised the manuscript, and read and approved the final draft.

Acknowledgements

This research is part of the U.S. Geological Survey (USGS) interdisciplinary research project, Future Impacts of Sea Level Rise on Coastal Habitats and Species (FISCHS), funded by the USGS Ecosystems Mapping, the USGS Greater Everglades Priority Ecosystems Science, and the USGS Climate and Land Use Change - Research and Development Program. FISCHS' team members, who were integrally involved in discussions on the development of the hindcast models, included Don DeAngelis, Ann Foster, Jiang Jiang, Melinda Lohmann, Thomas Smith, Brad Stith, and Zuzanna Zajac. Thomas Smith provided the surface-water salinity and stage data during Hurricane Wilma in 2005, which were used to validate the hydrological model.

Author details

[1]U.S. Geological Survey, Caribbean-Florida Water Science Center, 7500 SW 36th Street, Davie, FL 33314, USA. [2]U.S. Geological Survey, St. Petersburg Coastal and Marine Science Center, 600 Fourth Street South, St. Petersburg, FL 33701, USA. [3]U.S. Geological Survey, Southeast Ecological Science Center, 7920 NW 71st Street, Gainesville, FL 32653, USA.

Received: 1 August 2014 Accepted: 13 December 2014
Published online: 12 February 2015

References

Davis SE III, Cable JE, Childers DL, Coronado-Molina C, Day JW Jr, Hittle CD, Madden CJ, Reyes E, Rudnick D, Sklar F (2004) Importance of storm events in controlling ecosystem structure and function in a Florida Gulf coast estuary. J Coastal Res 20(4):1198–1208

Davis SM, Childers DL, Lorenze JJ, Wanless HR, Hopkins TE (2005) A conceptual model of ecological interations in the mangrove estuaries of the Florida Everglades. Wetlands 25(4):832

Fish GV (1930) Record rainfall for Miami, Florida. Mon Weather Rev 58(6):251–252

Green TW, Slone DH, Swain ED, Cherkiss MS, Lohmann M, Mazzotti FJ, Rice KG (2014) Evaluating effects of Everglades restoration on American crocodile populations in South Florida using a spatially-explicit, stage-based population model. Wetlands 34(Suppl 1):S213–S224

Guo W, Langevin CD (2002) User's guide to SEAWAT: a computer program for simulation of three-dimensional variable-density ground-water flow. In: Techniques of Water-Resources Investigations Book 6, Chapter A7

Heffernan JB, Soranno PA, Angilletta MJ, Buckley LB, Gruner DS, Keitt TH, Kellner JR, Kominoski JS, Rocha AV, Xiao J, Harms TK, Goring SJ, Koenig LE, McDowell WH, Powell H, Richardson AD, Stow CA, Vargas R, Weathers KC (2014) Macrosystems ecology: understanding ecological patterns and processes at continental scales. Front Ecol Env 12(1):5–14

Holland GJ (1980) An analytic model of the wind and pressure profiles in hurricanes. Mon Weather Rev 108(8):1212–1218

Hopkinson CS, Lugo AE, Alber M, Covich AP, Van Bloem SJ (2008) Forecasting effects of sea-level rise and wind storms on coastal and inland ecosystems. Front Ecol Env 6(5):255–263

Jiang J, DeAngelis DL (2013) Strong species-environment feedback shapes plant community assembly along environmental gradients. Ecol Evol 3(12):4119–4128, doi:10.1002/ece3.784

Jiang J, DeAngelis DL, Smith TJ, Teh SY, Koh HL (2012a) Spatial pattern formation of coastal vegetation in response to external gradients and positive feedbacks affecting soil porewater salinity: a model study. Landscape Ecol 27:109–119

Jiang J, Gao D, DeAngelis DL (2012b) Towards a theory of ecotone resilience: coastal vegetation on a salinity gradient. Theoretical Pop Ecol 82:27–37

Jiang J, DeAngelis DL, Anderson GH, Smith TJ III (2014) Analysis and simulation of propagule dispersal and salinity intrusion from storm surge on the movement of a marsh-mangrove ecotone in South Florida. Estuaries and Coasts 37:24–35, doi:10.1007/s12237-013-9666-4

Khairoutdinov MF, Emanuel KA (2013) Rotating radiative-convective equilibrium simulated by a cloud-resolving model. J Adv Model Earth Sys 5(4):816–825, doi:10.1002/2013ms000253

Landsea CW, Glenn DA, Bredemeyer W, Chenoweth M, Ellis R, Gamache J, Hufstetler L, Mock C, Perez R, Prieto R, Sánchez-Sesma J, Thomas D, Woolcock L (2008) A reanalysis of the 1911–20 Atlantic hurricane database. J Climate 21(10):2138–2168

Landsea CW, Feuer S, Hagen A, Glenn DA, Sims J, Perez R, Chenoweth M, Anderson N (2012) A reanalysis of the 1921-30 Atlantic hurricane database. J Climate 25(3):865–885

Langevin CD, Swain ED, Wolfert MA (2005) Simulation of integrated surface-water/groundwater flow and salinity for a coastal wetland and adjacent estuary. J Hydrol 314:212–234

Lohmann MA, Swain ED, Wang JD, Dixon J (2012) Evaluation of effects of changes in canal management and precipitation patterns on salinity in Biscayne Bay, Florida, using an integrated surface-water/groundwater model. US Geol Surv Sci Invest Rep 5009:94

Maul GA, Martin DM (1993) Sea level rise at Key West, Florida, 1846-1992: America's longest instrument record? Geophys Res Lett 20(18):1955–1958, doi:10.1029/93gl02371

Michener WK, Blood E, Bildstein K, Brinson M, Gardner L (1997) Climate change, hurricanes, and tropical storms, and rising sea level in coastal wetlands. Ecol App 7(3):770–801

Mitchell CL (1926) The West Indian hurricane of September 14-22, 1926. Mon Weather Rev 54(10):409–414

Obeysekera J, Browder J, Hornung L, Harwell MA (1999) The natural South Florida system I: climate, geology, and hydrology. Urban Ecosys 3:223–244

Obeysekera J, Kubler L, Ahmed S, Chang ML, Engel V, Langevin CD, Swain ED, Wan Y (2011) Use of hydrologic and hydrodynamic modeling for ecosystem restoration. Crit Rev Environ Sci Technol 41(1):447–488
Ogden JC, Davis SM, Jacobs KJ, Barnes T, Fling HE (2005) The use of conceptual ecological models to guide ecosystem restoration in South Florida. Wetlands 25 (4):795–809
Peters DPC, Bestelmeyer BT, Turner MG (2007) Cross-scale interactions and changing pattern-process relationships: consequences for system dynamics. Ecosys 10:790–796
Peterson GD, Cumming GS, Carpenter SR (2003) Scenario planning: a tool for conservation in an uncertain world. Con Biol 17(2):358–366
Pfost RL (2000) Operational tropical cyclone quantitative precipitation forecasting. Natl Weather Digest 24:61–66
Powell MD, Houston SH, Reinhold TA (1996) Hurricane Andrew's landfall in South Florida. Part 1: standardizing measurements for documentation of surface wind fields. Weather Forecast 11:304–328
Powell MD, Houston SH, Amat LR, Morisseau-Leroy N (1998) The HRD real-time hurricane wind analysis system. J Wind Eng Ind Aerodynamics 77&78:53–64
Renken RA, Dixon J, Koehmstedt J, Ishman S, Lietz AC, Marella RL, Telis P, Rogers J, Memberg S (2005) Impact of anthropogenic development on coastal ground-water hydrology in southeastern Florida, 1900-2000. US Geol Surv Circ 1275:77
Saha AK, Saha S, Sadle J, Jiang J, Ross MS, Price RM, Sternberg LSLO, Wendelberger KS (2011) Sea level rise and South Florida coastal forests. Climatic Change 107(1):81–108
Sheng YP, Paramygin VA (2010) Forecasting storm surge, inundation, and 3D circulation along the Florida coast. Estuarine Coastal Model 2009:744–761, doi:10.1061/41121(388)43
Smith TJ III, Tiling-Range G, Jones J, Nelson P, Foster A, Balentine K (2010) The use of historical charts and photographs in ecosystem restoration: examples from the Everglades Historical Air Photo Project. In: Cowley DC, Standring RA, Abicht MJ (eds) Landscapes through the lens: aerial photographs and the historic environment. Occ Pub Aerial Archaeology Res Group, vol No. 2. Oxbow Books, Oxford, UK. pp 179-191
Smith TJ III, Foster AM, Briere PR, Jones JW, Van Arsdall C (2002) Conversion of historical topographic sheets (T-sheets) from paper to digital form. U S Geological Survey Open-File Report 02-204, Florida Everglades and vicinity
Smoak JM, Breithaupt JL, Smith TJ, Sanders CJ (2013) Sediment accretion and organic carbon burial relative to sea-level rise and storm events in two mangrove forests in Everglades National Park. Catena 104:58–66, doi:10.1016/j.catena.2012.10.009
Stith BM, Reid JP, Langtimm CA, Swain ED, Doyle TJ, Slone DH, Decker JD, Soderqvist LE (2011) Temperature inverted haloclines provide winter warm-water refugia for manatees in southwest Florida. Estuaries Coasts 34:106–119
Swain ED (2005) A model for simulation of surface-water integrated flow and transport in two dimensions: user's guide for application to coastal wetlands. US Geol Surv Open-File Rep 1033:88
Swain ED, Decker JD (2010) Measurement-derived heat-budget approaches for simulating coastal wetland temperature with a hydrodynamic model. Wetlands 30(3):635–648, doi:10.1007/s13157-010-0053-7
Swain ED, James DE (2007) Inverse modeling of surface-water discharge to achieve restoration salinity performance measures in Florida Bay, Florida. J Hydrol 351:188–202
Swain ED, Lohmann MA, Decker JD (2008) Hydrologic simulations of water-management scenarios in support of the Comprehensive Everglades Restoration Plan. In: The role of hydrology in water resources management. IAHS Red Book Series, UNESCO/IAHS Symposium, October 2008, Isle of Capri, Napoli, Italy
Swain ED, Stefanova L, Smith TJ III (2014) Applying downscaled global climate model data to a hydrodynamic surface-water and groundwater model. Am J Clim Change 3(1):33–49, doi:10.4236/ajcc.2014.31004
Székely GJ, Rizzo ML, Bakirov NK (2007) Measuring and testing dependence by correlation of distances. Ann Stat 35(6):2769–2794
Teh SY, DeAngelis DL, Sternberg LSL, Miralles-Wilhelm F,R, Smith TJ, Koh H-L (2008) A simulation model for projecting changes in salinity concentrations and species dominance in the coastal margin habitats of the Everglades. Ecol Model 213:245–256
Wang JD, Swain ED, Wolfert MA, Langevin CD, James DE, Telis PA (2007) Application of FTLOADDS to simulate flow, salinity, and surface-water stage in the southern Everglades, Florida. US Geol Surv Sci Rep 5010:114
Weeks D, Malone P, Welling L (2011) Climate change scenario planning: a tool for managing parks into uncertain futures. Park Sci 28(1):26–33
Wilson AM, Moore WS, Boye SB, Anderson JL, Schutte CA (2011) Storm-driven groundwater flow in a salt marsh. Water Resources Res 47(W02535):1–11, doi:10.1029/2010WR009496
Zhang K, Xiao C, Shen J (2008) Comparison of the CEST and SLOSH models for storm surge flooding. J of Coastal Res 242:489–499
Zhang K, Liu H, Li Y, Xu H, Shen J, Rhome J, Smith TJ III (2012) The role of mangroves in attenuating storm surges. Estuar Coastal Shelf Sci 102–103:11–23